AWARD NUMBER: W81XWH-19-1-0660

TITLE: Multi-Omics and Mitochondrial Dysfunction in Acute Lung Injury

PRINCIPAL INVESTIGATOR: Madesh Muniswamy, Ph.D.

CONTRACTING ORGANIZATION: The Univ. of TX Hlth Sci Ctr at San Antonio

REPORT DATE: OCTOBER 2021

TYPE OF REPORT: Annual Technical Report

PREPARED FOR: U.S. Army Medical Research and Development Command
Fort Detrick, Maryland 21702-5012

REPORT DOCUMENTATION PAGE

Form Approved
OMB No. 0704-0188

1. REPORT DATE	**2. REPORT TYPE**	**3. DATES COVERED**
OCTOBER 2021	Annual Technical Report	09/01/2020-08/31/2021

4. TITLE AND SUBTITLE

Multi-Omics and Mitochondrial Dysfunction in Acute Lung Injury

5a. CONTRACT NUMBER
W81XWH-19-1-0660

5b. GRANT NUMBER
PR181598P1

5c. PROGRAM ELEMENT NUMBER

6. AUTHOR(S)

Madesh Muniswamy, Ph.D.

E-Mail: muniswamy@uthscsa.edu

5d. PROJECT NUMBER

5e. TASK NUMBER

5f. WORK UNIT NUMBER

7. PERFORMING ORGANIZATION NAME(S) AND ADDRESS(ES)

The University of Texas Health Science Center at San Antonio
7703 Floyd Curl Drive
San Antonio, Texas 78229-3900

8. PERFORMING ORGANIZATION REPORT NUMBER

8007721620000

9. SPONSORING / MONITORING AGENCY NAME(S) AND ADDRESS(ES)

U.S. Army Medical Research and Development Command
Fort Detrick, Maryland 21702-5012

10. SPONSOR/MONITOR'S ACRONYM(S)

11. SPONSOR/MONITOR'S REPORT NUMBER(S)

12. DISTRIBUTION / AVAILABILITY STATEMENT

Approved for Public Release; Distribution Unlimited

13. SUPPLEMENTARY NOTES

14. ABSTRACT

This proposal addresses the FY18 PRMRP Topic Area of "Acute Lung Injury", utilizing novel approaches (metabolomics, lipidomics, and mass spec imaging) to identify the causes of sepsis-induced acute lung injury (ALI) and biomarkers which differentiate patients at risk of developing ALI from those not at risk. This project also proposes the development and testing of a potential new drug, BTP2, to reduce the incidence and/or severity of ALI.

15. SUBJECT TERMS

ATP – adenosine triphospate; mCa2+ – mitochondrial Ca2+; MCU – mitochondrial Ca2+ uniporter; ROS – reactive oxygen species

16. SECURITY CLASSIFICATION OF:			**17. LIMITATION OF ABSTRACT**	**18. NUMBER OF PAGES**	**19a. NAME OF RESPONSIBLE PERSON**
a. REPORT	**b. ABSTRACT**	**c. THIS PAGE**			USAMRDC
Unclassified	Unclassified	Unclassified	Unclassified	15	**19b. TELEPHONE NUMBER** *(include area code)*

Standard Form 298 (Rev. 8-98)
Prescribed by ANSI Std. Z39.18

Table of Contents

REPORT OUTLINE

1. **INTRODUCTION:**

Multiple organ failure (MOF) is a major cause of death and reduced quality of life in the military theater and in civilian life. Causes include blunt trauma and shock-like states leading to ischemia and inflammation and impaired cellular function in multiple tissues. Limited mechanisms and tools are currently available to understand the progression of sepsis and trauma to ALI due to heterogeneity in patient populations. Our recent findings revealed that LPS-induced vascular permeability is initiated by LPS-induced overproduction of reactive oxygen species (ROS), which in turn leads to Ca^{2+} transients via modulation of both InsP3-dependent Ca^{2+} release and extracellular Ca^{2+} influx through STIM/Orai1. The resultant elevation in cytoplasmic Ca^{2+} leads to further mitochondrial Ca^{2+} overload via the mitochondrial Ca^{2+} uniporter (MCU), creating a positive feedback loop leading to the expression of multiple inflammatory molecules (lipids, metabolites, proteins) that contribute to vascular leakage and ultimately, to MOF. One of the major changes that occur during Multi-organ-failure (MOF) in severe sepsis is mitochondrial dysfunction. Under aerobic conditions, energy conserving molecules produced in the Tri-Carboxylic Acid cycle are utilized by the Electron Transport Chain to produce ATP in a process known as oxidative phosphorylation (OXPHOS). During sepsis, OXPHOS can become impaired, and organs rich in mitochondria become highly susceptible to injury. While oxygen deprivation is known to compromise mitochondrial function, it remains poorly understood how ion channels like MCU may act as a regulator of organ function during sepsis. To identify and establish the components that participate in LPS-mediated mitochondrial reprogramming and MOF, we will utilize multiple innovative approaches including, the newly designed small molecule MCU inhibitor, MCU knockout (***Cell Reports 2016***), CRISPR/Cas9-mediated MCU knock-in (***Cell Reports 2019***) mouse models, and multiomic tools coupled with systems biology.

2. **KEYWORDS:**

ALI – acute lung injury
ATP – adenosine triphospate
$[Ca^{2+}]_m$ – mitochondrial calcium concentration
$[Ca^{2+}]_c$ – cytosolic calcium concentration
CFU – colony forming units
EC – endothelial cell
ICAM 1 – intracellular adhesion molecule 1
KI – knock in
KO – knockout
LPS – lipopolysaccharide
$_mCa^{2+}$ – mitochondrial Ca^{2+}
MCU – mitochondrial Ca^{2+} uniporter
MPMVECs – mouse primary microvascular endothelial cells
mROS – mitochondrial reactive oxygen species
OCR – oxygen consumption rate
Orai1 – Calcium Release-Activated Calcium Modulator 1
OxPhos – oxidative phosphorylation
ROS – reactive oxygen species
SOCE – store-operated calcium entry
VE-cre – transgenic mouse strain expression cre-recombinase under the vascular endothelial-cadherin promoter

3. **ACCOMPLISHMENTS:**

a. **What were the major goals of the project?**

Major Task 1 Measure $[Ca^{2+}]_m$ and $[Ca^{2+}]_c$ transients, mitochondrial membrane polarization, OCR, cellular ATP levels, endothelial migration by scratch assay and EC cell death in BTP2-treated, control, and MCU^{C96A} KI endothelial cells.

Major Task 2 Assessment of intracellular and extracellular metabolite and lipid profiles in ECs following LPS challenge.

Major Task 3 Investigate the role of Orai and MCU in vascular neutrophil transmigration and lung vascular permeability in LPS-induced ALI

Major Task 4 Assessment of intracellular and extracellular metabolite and lipid profiles in ECs following LPS challenge.

During the Year 2, we have accomplished specific Aim 1C-1E. We have also started Aim 2.

b. **What was accomplished under these goals?**

During the Year 2, we have accomplished specific Aim 1C-1E. We have also started Aim 2A.

Accomplishments:

Increase in intracellular Ca^{2+} ($[Ca^{2+}]_i$) levels regulates cytokine production and plays a central role in EC function. In macrophage cells, release of Ca^{2+} from the internal ER stores, leads to the activation of SOCE mechanism. Similarly, agonist binding to the cell surface receptors generates second messenger (IP_3) that induces the release of Ca^{2+} from the ER. Once ER Ca^{2+} stores are depleted, Stromal Interaction Molecule 1 (STIM1), which acts as an ER Ca $^{2+}$ sensor, aggregates and activates the plasma membrane Ca^{2+} influx channels. Importantly, two distinct Ca^{2+} influx channels, Ca^{2+} release-activated Ca^{2+} channel (Orai1) and Transient Receptor Potential Canonical 1 (TRPC1) channels have been shown to interact with STIM1 to raise $[Ca^{2+}]_i$.

Loss of Orai1 expression results in loss of M2 phenotype development even with IL-4 stimulus:

We next evaluated the physiological effect of Orai1 Ca^{2+} entry channels on Mφ cell transition. Naïve Mφ, M1, and M2 cells were transfected with non-targeting siRNA (SiC, for control) or Orai1siRNA (siOrai1) to evaluate its role in their activation. Silencing of Orai1 in naïve Mφ cells displayed nominal expression of the classical $F4/80^+CD11b^+$ markers, when compared to control siRNA treated cells (Fig.1**A, B**). In contrast, activated M1 cells were not significantly affected by the transfection of siOrai1 and were able to maintain the same levels of M1 surface markers (CD80+CD86) (Fig. 1**C, D**). Nevertheless, activated M2 cells transfected with siOrai1 had considerably low levels of M2 phenotype markers (Fig.1**E-F**). To demonstrate the role of Orai1 in Mφ cells from $Orai^{fl/fl}$ mice were obtained and were treated with Ad.Cre virus to knockdown Orai1 expression (not shown). Loss of Orai1 significantly reduced cell viability in naïve Mφ and M2 cells, without affecting the M1 phenotype cells (Fig.1**G**). Flow cytometry further showed no significant difference in the M1 surface markers, however, a significant decrease in the level of M2 markers was observed in $Orai^{flfl}$ mice cells that was treated with Ad.Cre. (Fig.1**H, I**). ELISA analysis of supernatants from M2 cells from $Orai1^{fl/fl}$ + Ad.Cre virus mice displayed a significant decrease in anti-inflammatory cytokine IL-10, as compared to control cells (no Ad.Cre virus) (Fig.1**I**). Interestingly, lack of Orai1 did not affect cytokines associated with M1 phenotype (Fig.1**I**). Immunoblot analysis of the markers for M1 and M2 phenotype, showed no increase of iNOS expression once the Orai1 gene was inactivated (Fig. 1**J** Fig. S5B). In contrast, significant decrease in Arginase1 expression was observed in M2 activated cells of $Orai1^{-/-}$ (Fig. 1**J**).

Functional characterization of the channel activity also showed that loss of Orai1, only affected the naïve and the M2 phenotype, whereas no change in the Ca^{2+} currents in the M1 phenotype was observed (Fig. 1**K**). Although it has been established that agonist induced Ca^{2+} release and SOCE are essential for mitochondrial Ca^{2+} uptake, it remains unclear

whether Orai-mediated Ca^{2+} entry modulates mitochondrial bioenergetics. To evaluate the mitochondrial bioenergetics, we measured the oxygen consumption rate (OCR) of the naïve Mφ, pro-inflammatory (M1) and anti-inflammatory (M2) macrophages derived from wild-type mice. 48 hours cultured M0 macrophages exhibited low basal and maximal OCR. While macrophages treated with IFNγ (20 ng/ml) or IL-4 (20 ng/ml) showed higher basal and maximal OCR (Fig. 1**L,**

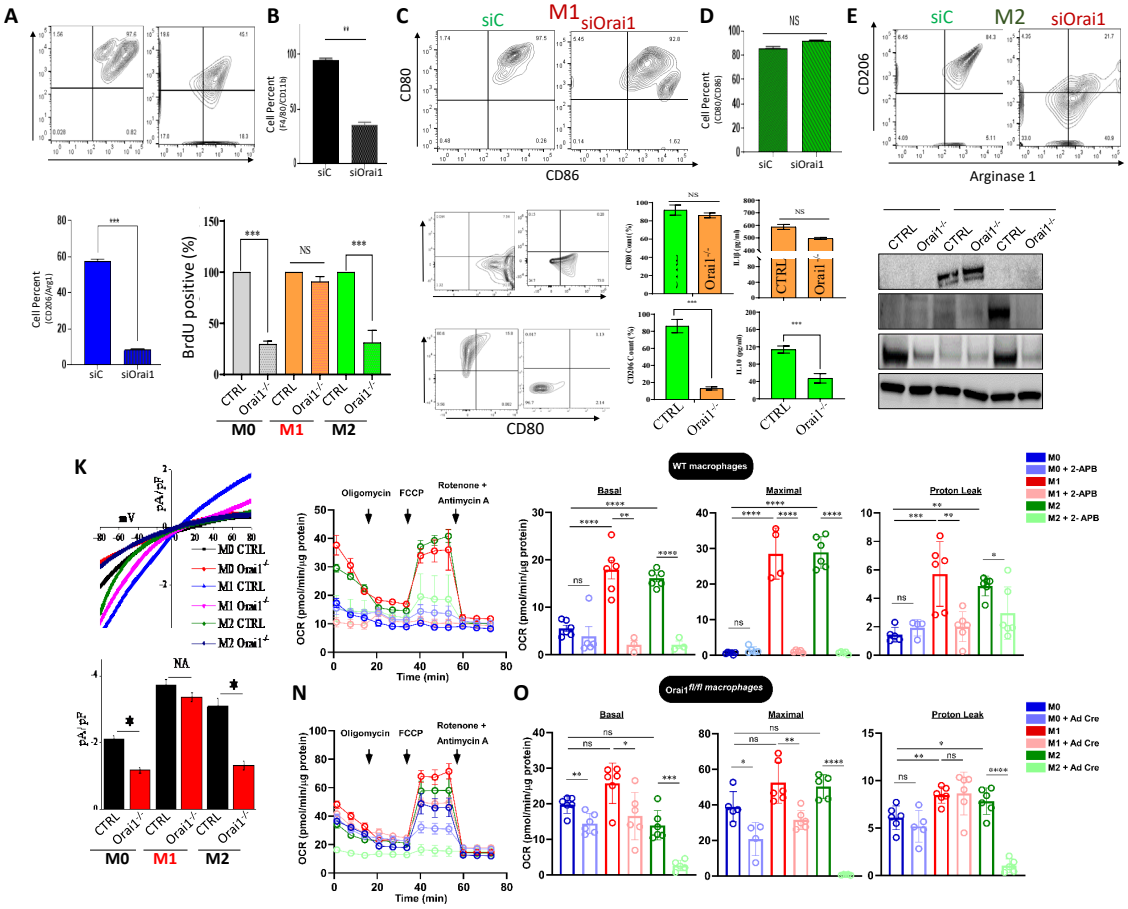

Fig.1. Lack of Orai1 results in impaired M2 phenotype development even with IL4 stimulus. Flow cytometric analysis of macrophage polarization in controlsiRNA (siC) and siOrai1 treated cells. BMDM cells were harvested after 24hr after gene silencing and flow cytometry was performed to measure the levels of $F4/80^+$ and $CD11b^+$. Data shown are representative of three independent experiments with similar results. Percentage of positive cells for $F4/80^+$ and $CD11b^+$ under the conditions in Fig. 1**A**. Data shown are representative of three independent experiments with similar results. Bar graphs depicts average ± SD for relative values, $^{**}p \leq 0.001$ (Student's t test). Flow cytometric analysis ($CD80^+$ and $CD86^+$) on macrophage upon respective siRNA treatment. Data shown are representative of three independent experiments. Percentage of CD80+ and CD86+ positive cells. Bar graphs depicts average ± SD for relative values, NS = non-significant (Student's t test) from 2 independent experiments. Flow cytometric analysis of $CD206^+$ and Arginase 1^+ upon Orai1 silencing. Data shown are representative of three independent experiments with similar results. Percentage of positive cells for M2 markers of ($CD206^+$ and $Arginase1^+$). Data shown are representative of three independent experiments. Bar graphs depicts average ± SD for relative values, $^{***}p \leq 0.001$, NS = non-significant (Student's t test). Cell proliferation assay for $Orai^{fl/fl}$ with (for $Orai1^{-/-}$) and without (CTRL) Ad.Cre virus. Data shown are representative of three independent experiments. Bar graphs depicts BrdU positive cells ± SD for positive cells, $^{***}p \leq 0.001$ (Student's t test), NS=non-significant. n = 3 to 4 independent replicates. Flow cytometer analysis to measure the difference between $Orai1^{fl/fl}$ with and without Ad.Cre virus for M1, M2 markers. Data shown are representative of three independent experiments. Percentage of positive cells for CD80 and CD206 under the conditions in Fig. 5H. Data shown are representative of three independent experiments with similar results. Bar graphs depicts average ± SD for relative values, NS = non-significant, $^{***}p \leq 0.001$ (Student's t test). Immunoblot analysis showing the level of expression of iNOS, Arginase1, Orai1, and β-actin of control and $Orai1^{fl/fl}$ mice with and without Ad.Cre virus. Data shown are representative of three independent experiments with similar results. IV curves of Tg-induced currents at - 80mV in $Orai1^{fl/fl}$ with and without Ad.Cre virus in various cells. Bar graphs represent quantitation (6-8 recordings for each condition) of current intensity at -80mV. $^{*}p \leq 0.05$ (Student's t test). Oxygen Consumption Rate (OCR) was analyzed in macrophages isolated from WT with and without 2APB (50 µM for 6 hrs) or from WT and $Orai1^{fl/fl}$ macrophages treated with Ad5a iCre for 72 hours for M0, M1 and M2 phenotypes. N=3 performed in duplicate. Basal, maximal respiration and proton leak analysis of macrophages isolated from WT with and without 2APB (50 µM for 6 hrs) WT and $Orai1^{fl/fl}$ macrophages treated with Ad5a iCre for 72 hours. Mean ±SEM, n=3, $^{*}p < 0.05$, $^{**}p < 0.01$, $^{***}p < 0.001$, $^{****}p < 0.0001$. n.s., not significant.

M). Upon pretreatment with SOCE blocker 2-APB (50 µM), the basal and maximal OCR were significantly suppressed in M1 and M2 macrophages (Fig. 1**L, M**). Since 2APB effect is nonselective, we next tested whether genetic ablation of Orai1 in macrophages alters mitochondrial OCR. $Orai1^{fl/fl}$ macrophages were infected with Ad.Cre virus for 72 hours. After 48 hours of Cre virus infection naïve Mφ from WT and $Orai1^{fl/fl}$ mice were polarized to become pro-inflammatory

macrophages (M1) and anti-inflammatory macrophages (M2) upon IFNγ or IL-4 stimulation for 24 hours. After polarization, mitochondrial OCR was measured. The M1 and M2 macrophages exhibited higher basal and maximal respiration states compared to the naïve Mφ (Fig. 1**N, O**). However, loss of Orai1 showed remarkably lower levels of mitochondrial OCR (basal and maximal) especially in the M2 phenotype (Fig.1**O**). Collectively, these data indicate that inhibition of SOCE or loss of Orai1 prevents mitochondrial bioenergetics possibly through preventing mitochondrial Ca^{2+} uptake mechanism that further modulate macrophage polarization.

Deletion of Orai1 promotes macrophage mitochondrial shape transition

Having observed remarkable changes in mitochondrial OCR, we next assessed whether there is a link between mitochondrial morphology and bioenergetics. Orai1$^{fl/fl}$ macrophages were infected with Ad.Cre virus for 72 hours. After

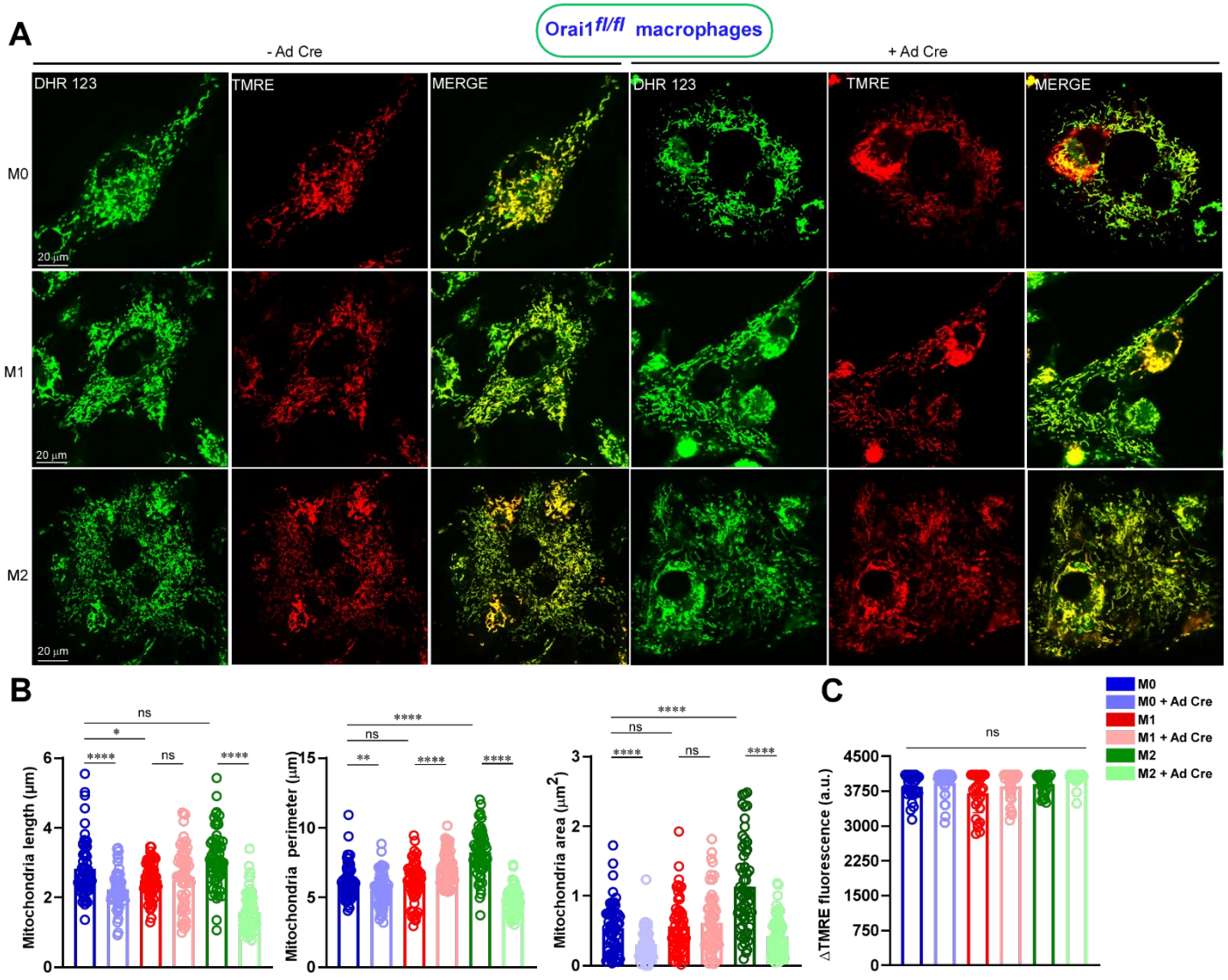

Fig. 2. Orai1 deletion exhibits macrophage mitochondrial shape transition. (**A, B**) Mitochondrial phenotype was assessed in macrophages derived from Orai1$^{fl/fl}$ mice with and without Ad5a iCre treatment for 72 hours. Macrophages were stained with DHR123 and TMRE for 30 minutes and confocal images were acquired immediately. Images shown are representative of 3 independent experiments. Quantification (Mean ±SEM) of mitochondrial length, perimeter and mitochondrial area are shown as bar graph. *p < 0.05, **p < 0.01, ***p < 0.001, ****p < 0.0001. n.s., not significant. (**C**) Measurement of mitochondrial membrane potential as TMRE fluorescence retention in the mitochondria. Mean ±SEM, n=3, n.s., not significant.

48 hours of Cre virus infection, naïve Mφ from WT and Orai1$^{fl/fl}$ mice were polarized and mitochondrial morphology was assessed by confocal imaging. The polarized M1 and M2 macrophages exhibited characteristically distinct phenotypic variations in mitochondria length, area and perimeter, when compared to naïve Mφ (Fig.2**A, B**). In comparison to uninfected macrophages, naïve and M2, but not M1 macrophages, infected with the Ad.Cre virus showed a marked reduction in mitochondria length and area (Fig.1**A, B**). Significant variations in the mitochondrial perimeter, but not in mitochondrial length and area, demonstrated that the mitochondrial shape transition events linearly affected mitochondrial OCR and bioenergetics. However, mitochondrial membrane potential (ΔΨm) of the uninfected and

Ad.Cre virus infected naïve Mφ, M1, and M2 macrophages were similar (Fig. 2**C**). The results strongly suggest Orai1-mediated Ca^{2+} entry is crucial for mitochondrial bioenergetics in naïve Mφ and in the activation of the M2 phenotype.

Alterations in SOCE channel expression dictates M1/M2 transformation

The results presented thus far suggest that Orai1 is essential for the M2 phenotype, but did not affect M1 phenotype, which is dependent on TRPC1 function. Thus, next, we evaluated if alterations in the expression of these Ca^{2+} entry channels (Orai1 and TRPC1) could modulate the M1 and M2 transition and establish its role in macrophage heterogeneity and plasticity. To achieve our objective, we transfected with respective siRNA and at the same time overexpressed the alternate Ca^{2+} entry channel and compared the production of proinflammatory M1 and anti-inflammatory M2 cytokines. IFNγ activated M1 cells were transfected with siRNA that targets TRPC1 (siTRPC1), along with a plasmid that overexpress Orai1 gene. Importantly, IL-6 and IFNγ (that indicates M1 phenotype) levels were significantly lower in supernatants of M1 activated cells that overexpress Orai1 but were silenced for TRPC1 (Fig.3**A**). In contrast, cytokines that are classical for M2 activation (IL-10 and IL1RII) levels were increased in cells

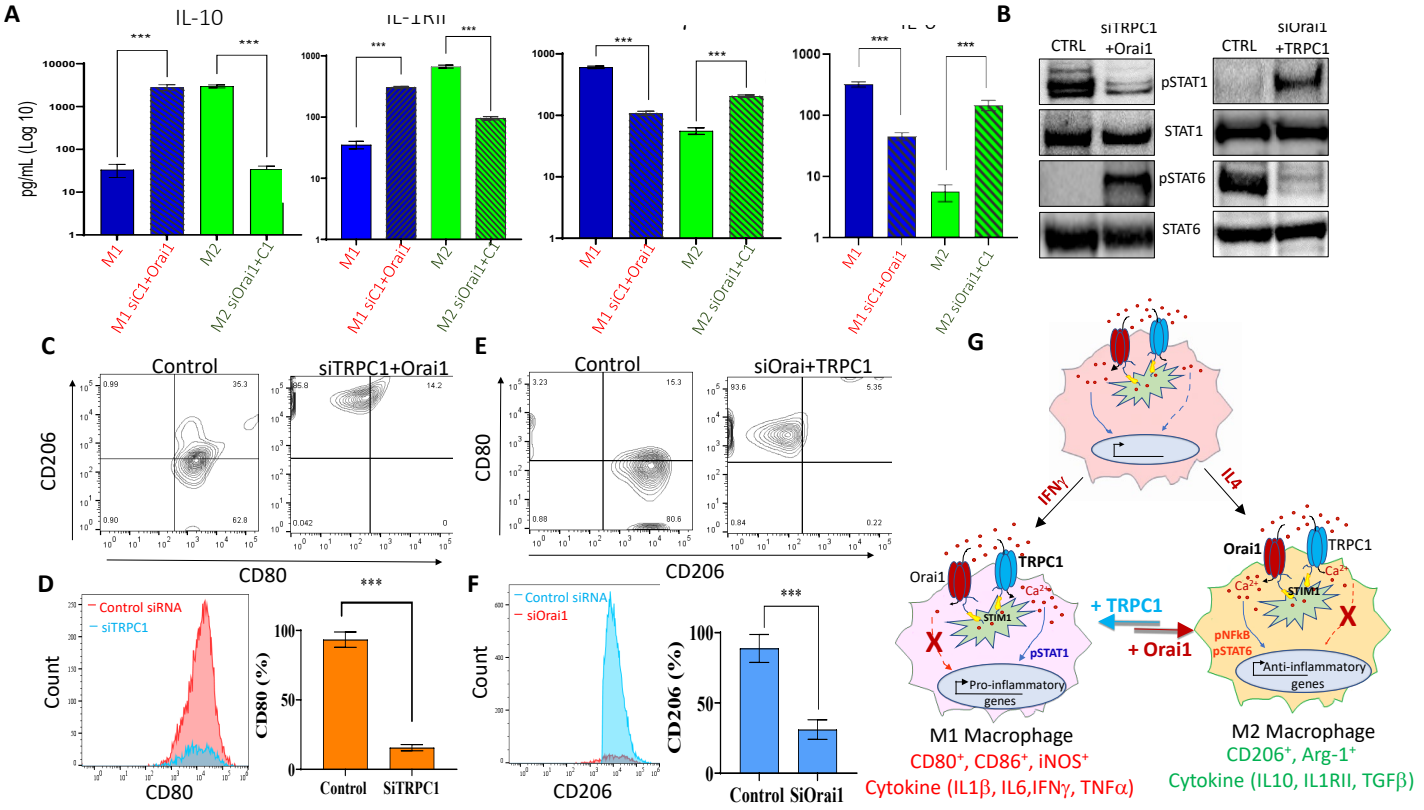

Fig. 3. Ca^{2+} influx via TRPC1 channels mediate M1 phenotype polarization and M2 polarization is dependent on Orai1 channels. (**A**) Cytokine released in M1 (+IFNγ for 24hr) cells along with silencing of TRPC1 and overexpressing Orai1 and in M2 (+IL-4 for 24 hr) cells in Orai1 silenced cells, but overexpressing TRPC1 gene was measured by ELISA. Data shown are representative of three independent experiments. Bar graphs depicts average ± SD for relative values, ***$p \leq 0.001$ (Student's t test). (**B**) Immunoblot analysis showing the level of expression of pSTAT1, STAT1, pSTAT6 and STAT6 in conditions as labeled. Data shown are representative of three independent experiments. (**C-F**) Flow cytometry analysis of cells listed in Fig 5A to measure levels of M1 ($CD80^+$) and M2 markers ($CD206^+$) in various conditions. Data shown are representative of three independent experiments. Percentage of positive cells for M1 ($CD80^+$) and M2 ($CD206^+$) under the conditions are shown as bar graph depicting average ± SD for relative values, ***$p \leq 0.001$ (Student's t test). Data shown are representative of three independent experiments. (**G**) Schematic overview showing that macrophage polarization is dependent on individual Ca^{2+} channels activation.

that overexpressed Orai1 and were silenced for TRPC1 (Fig. 3**A**). Similarly, IL-4 activated M2 cells were transfected with Orai1siRNA along with TRPC1 overexpression, which displayed high levels of M1 related cytokines and low levels of M2 cytokines (Fig. 3**A**). Consistent with these results, immunoblot analysis showed a significant decrease in the phosphorylation of pSTAT1, without any significant change in total STAT1 levels in TRPC1 silenced, but Orai1 overexpressed cells (Fig. 3**B**). In contrast, a significant increase in the phosphorylation of STAT6 was observed upon TRPC1 silenced, but Orai1 overexpressed cells (Fig.7B**,** Fig.S5C). Similarly, decrease in Orai1 along with an increase in TRPC1 expression, increased pSTAT1 phosphorylation, along with a decrease in pSTAT6 phosphorylation (Fig. 3**B**). Interestingly, flow cytometry analysis also showed that in M1 activated cells, which were transfected with siTRPC1 and overexpress Orai1, displayed reduced surface M1 marker (CD80), in conjunction with an increase in M2 marker

(Fig. 3**C, D**). Correspondingly, M2 activated cells transfected with siOrai1 along with TRPC1 overexpression also displayed significantly lower levels of M2 marker (CD206), while showing high levels of M1 marker (CD80) (Fig. 3**E, F**). Together these results demonstrate that TRPC1 channels play key role in the development of the IFNγ-induced M1 functional phenotype, whereas Orai1 is critical for IL4-induced M2 phenotype. Moreover, alterations in their expression dictates the M1 to M2 or M2 to M1 transformation, which establish a clear separation of essential Ca^{2+} influx channels and identify novel mechanisms that could lead to macrophages transformation by altering the expression of the SOCE channels (Fig. 3**G**).

Methodology:

Protein Extractions and Western blotting

Protein lysates were prepared in lysis buffer (10mM Tris,140mMNaCl,1%NP-40, 0.5% SDS, and protease inhibitors, pH 8.0), protein concentrations were determined, using the Bradford reagent (Bio-Rad Laboratories, Hercules, CA, USA), and 25–50 ug of proteins were resolved on NuPAGE Novex 4–12% BisTris gels, transferred to PVDF membranes The membrane was blocked with skim milk in PBST solution and incubated with primary antibodies. After washing with PBST, secondary antibodies were applied and detected by the Clarity Max Western ECL Substrate (Bio-Rad Laboratories, Hercules, CA, USA). Densitometric analysis was performed using ImageJ analysis and results were corrected for protein loading by normalization for β-actin (Cell Signaling, 4970S) as previously described (*55*). Blot stripping was performed whenever necessary, using Restore PLUS Western Blot Stripping Buffer (Thermo Fisher, Waltham, MA, USA). The blots were washed with PBS Tween 20 (Sigma, St. Louis, MO, USA), then immersed in stripping buffer for 15mins at room temperature, washed again and blocked for another 30 minutes before incubation with the new antibody. The following primary antibodies (dilution accordingly by manufacturer's protocol) were used for western blot analysis: anti-STIM1 (Cell Signaling, D88E10), anti-Orai1 (Thermo-Fisher, PA5-26378), anti-Orai2 (Abcam, ab180146), anti-Orai3 (Abcam, ab254260), anti-TRPC1 (Alamone, ACC-010), anti-TRPC3 (ThermoFisher, PA577307), anti-STIM1 (Cell Signaling, 5668S), anti-STIM2 (Cell Signaling, 4917S), anti-JNK (Cell Signaling, 9252), anti-pJNK (Thr81) (Cell Signaling, 2676), anti-NFκB (p65) (Cell Signaling, 8242S), anti- pNFκB p65 (pp65) (Cell Signaling, 3033S), anti-STAT1 (Cell Signaling, 14994S), anti-pSTAT1 (Cell Signaling, 9167S), anti-STAT6 (Cell Signaling, 5397S), anti-pSTAT6 (Cell Signaling, 56554S), anti-iNOS (Cell Signaling, 13120S), anti-Arginase 1 (Cell Signaling, 93668S), Goat anti-rabbit (Cell Signaling, 7074S) and goat anti-mouse (Cell Signaling, 7076S) IgGs were used as secondary antibodies.

Measurement of cytokines levels

IL-6, TNF-α, and IL-1β levels in the supernatant were measured using the Enzyme-Linked ImmunoSorbent Assay (ELISA) kit (Life Technologies, Carlsbad, CA, USA) following the manufacturer's instructions using standard diluent buffers designed for use with mouse serum. We use Lipopolysaccharides (LPS 100ng/ml, Sigma, St. Louis, MO, USA) as a positive control, cells were incubated for 3hrs after treatments. HMGB1, Histone 3 and hsp70 levels were measured by direct Elisa by self-coating protocol, previously described. All samples were measured on a single 96-well plate for each cytokine, the cultured medium was centrifuged at 800 G at for 5 min 4°C and the supernatant was used as the sample. Based on that criterion, all cytokine values for the murine cell line Raw 264.7 and bone marrow-derived macrophages serum samples examined were above the limit of detection and within the reportable range of each assay.

Flow cytometry

On day 7, formation of mature BMDM is evaluated using flow cytometry analysis and fluorophore conjugated antibodies. Cells were resuspended with FACS buffer (PBS supplemented with 0.2% BSA), then blocked with Anti-Mouse CD16/CD32 Fc Blocker (BD Pharmigen, San Jose, CA, USA) for 15 minutes. After blocking, cells were tested for the expression of Anti-CD11b antibody [M1/70] (PE/Cy5®) (Abcam, Burlingame, CA, USA) and F4/80 Monoclonal Antibody (BM8), Pacific Blue (Thermo Fisher, Waltham, MA, USA) for macrophage line confirmation. For M1 macrophages, cells were stained with Anti-Mouse

CD80 PE (eBioscience, San Diego, CA, USA) and Anti-Mouse iNOS Alexa Fluor 488 (eBioscience, San Diego, CA, USA); for M2 macrophage cells were stained with Anti-Mouse Arginase 1 PE-Cyanine (eBioscience, San Diego, CA, USA) and Anti-Mouse CD206 APC (eBioscience, San Diego, CA, USA). Cells were incubated for for 30 min at 4°C, then quantified on a BD LSR II (BD Pharmigen, San Jose, CA, USA).

Measurement of Mitochondrial oxygen consumption rate

Bone Marrow Derived Macrophages (BMDM) from WT and Orai1$^{fl/fl}$ mice (n=3) were plated on 96 well Agilent Seahorse XF Cell culture microplates at a density of 4 x 10^5 cells per well. The macrophages were plated in their normal growth media overnight. The plated Orai1$^{fl/fl}$ macrophages were infected with Adeno-Cre virus (Ad) mediated Cre deletion for floxed sequences (20 MOI) for 72 h. After 48 hours of Cre virus infection, naive macrophages (M0) from WT and Orai1$^{fl/fl}$ mice were polarized to become pro-inflammatory macrophages (M1) and anti-inflammatory macrophages (M2) upon Interferon-γ (IFNγ) or interleukin-4 (IL-4) stimulation for 24 hours. After polarization, the media was changed to Seahorse XF Cell Mito Stress Test Kit (Agilent) assay media supplemented with glucose, glutamine, pyruvate concentrations equivalent to that of the growth media. Naïve Mφ, M1 and M2 macrophages were treated with the SOCE channel inhibitor, 2ABP (50 μM) for 15 minutes and oxygen consumption rate (OCR) was measured at 37°C in an XF96 extracellular flux analyzer (Seahorse Bioscience, Agilent), which had been previously calibrated using Seahorse XF Calibrant solution (Seahorse Bioscience, Agilent) in a CO_2-free incubator overnight. Respiratory chain inhibitors were then loaded into the XF96 flux analyzer and added sequentially to cells at indicated time points. M0, M1 and M2 macrophages received oligomycin (2 μM), FCCP (5 μM), and a mixture of antimycin A and rotenone (1 μM) sequentially. Data were collected using Agilent Seahorse Wave 2.6.1 Desktop software and exported to GraphPad Prism version 8 for analysis.

Measurement of Mitochondrial morphology and membrane potential

BMDM from Orai1$^{fl/fl}$ mice were plated on 35 mm MatTek dishes, in normal growth media. The plated Orai1$^{fl/fl}$ macrophages were infected with adeno-Cre virus (20 MOI) and after 48 hours of Cre virus infection, naive macrophages (M0) from WT and Orai1$^{fl/fl}$ mice were polarized to become pro-inflammatory macrophages (M1) and anti-inflammatory macrophages (M2) upon IFNγ or IL-4 stimulation for 24 hours. The mitochondrial morphology and the $\Delta\Psi_m$ were determined after staining with dihydrorhodamine 123 (2.5 μM) (ex/em 505/524 nm) and Tetramethylrhodamine, ethyl ester, perchlorate (TMRE; 100 nM; ex/em 556/610 nm) at room temperature) for 30 minutes. The stained macrophages were washed and imaged using Leica SP8 Confocal microscope (Manheim, Germany) coupled with a temperature-controlled environmental chamber. The images were acquired, and mitochondrial length, area and perimeter were quantified using the Leica Application Suite X software and analyzed using GraphPad Prism version 8.

c. **What opportunities for training and professional development has the project provided?**

Nothing to Report

d. **How were the results disseminated to communities of interest?**

Nothing to Report

e. **What do you plan to do during the next reporting period to accomplish the goals?**

We will comprehensively analyze changes in metabolites and lipids from cell extracts and conditioned media from endothelial cells of Control (VE-Cre) and KO (Orai1ΔEC and MCUΔEC) mice before and after LPS treatment. Upon completion of **Aim 1**, we will test and define whether MCU as a critical regulator of EC survival and vascular inflammation during sepsis (**Aim 2**). Here, our goal is to establish the in vivo relevance of this relationship towards control of pathogen-induced pulmonary vascular dysfunction. K.

pneumoniae is a gram-negative bacterium that causes respiratory infections in human and animal hosts and produces significant quantities of LPS, which is thought to be a major factor in ALI. To assess the role of SOCE and MCU-dependent Ca^{2+} signaling in triggering vascular inflammation and lung injury experiments in this sub-aim will focus on studying the response of mice exhibiting EC-specific loss of Orai1 and MCU to K. pneumoniae. To test our hypothesis, we will use Orai1 and MCU EC KO mice which will demonstrate whether these mice are susceptible or resistant to bacterial infection.

4. **IMPACT:**
    a. **What was the impact on the development of the principal discipline(s) of the project?**

Nothing to Report

    b. **What was the impact on other disciplines?**

Nothing to Report

    c. **What was the impact on technology transfer?**

Nothing to Report

    d. **What was the impact on society beyond science and technology?**

Nothing to Report

5. **CHANGES/PROBLEMS:**
    a. **Changes in approach and reasons for change**

Nothing to report. .

    b. **Actual or anticipated problems or delays and actions or plans to resolve them**

Nothing to Report

        i.
    c. **Changes that had a significant impact on expenditures**

Nothing to Report

    d. **Significant changes in use or care of human subjects, vertebrate animals, biohazards, and/or select agents**

Nothing to report.

    e. **Significant changes in use or care of human subjects**

Nothing to Report

    f. **Significant changes in use or care of vertebrate animals.**

Nothing to Report

g. **Significant changes in use of biohazards and/or select agents**

Nothing to Report

6. **PRODUCTS:**

Publications, conference papers, and presentations

- **Journal publications.**

1. Cassidy C. Daw, Karthik Ramachandran, Benjamin T. Enslow, Soumya Maity, Brian Bursic, Matthew J. Novello, Cherubina S. Rubannelsonkumar, Ayah H. Mashal, Joel Ravichandran, Terry M. Bakewell, Weiwei Wang, Kang Li, Travis R. Madaris, Christopher E. Shannon, Luke Norton, Soundarya Kandala, Jeffrey Caplan, Subramanya Srikantan, Peter B. Stathopulos, **W. Brian Reeves,** Muniswamy Madesh. Lactate elicits ER-mitochondrial Mg^{2+} dynamics to integrate cellular metabolism. **Cell** 2020 Oct 15;183(2):474-489.e17. PMID: 33035451 PMCID: PMC7572828

2. B Rita Alevriadou, Akshar Patel, Megan Noble, Sagnika Ghosh, Vishal M Gohil, Peter B Stathopulos, Muniswamy Madesh*. Molecular nature and physiological role of the mitochondrial calcium uniporter channel. **Am J Physiol Cell Physiol.** 2021 Apr 1;320(4):C465-C482 (Invited Review).

3. Neelanjan Vishnu, Justin Wilson, Muniswamy Madesh. Emergence of repurposed drugs as modulators of MCU channel for clinical therapeutics. **Cell Calcium** (In press) 2021.

4. Lee HJ, Donati A, Feliers D, Sun Y, Ding Y, Madesh M, Salmon AB, Ikeno Y, Ross C, O'Connor CL, Ju W, Bitzer M, Chen Y, Choudhury GG, Singh BB, Sharma K, Kasinath BS. Chloride channel accessory 1 integrates chloride channel activity and mTORC1 in aging-related kidney injury. **Aging Cell.** 2021 Jul;20(7):e13407.

- **Books or other non-periodical, one-time publications.**

Nothing to report.

- **Other publications, conference papers, and presentations.**

Nothing to report.

Website(s) or other Internet site(s)

Nothing to report

Technologies or techniques

Nothing to report

Inventions, patent applications, and/or licenses

Nothing to report

Other Products

Nothing to Report

7. **PARTICIPANTS & OTHER COLLABORATING ORGANIZATIONS**
   a. **What individuals have worked on the project?**

Name:	Madesh Muniswamy (no change)
Project Role:	PI
Researcher Identifier (e.g. ORCID ID):	0000-0001-6745-9092
Nearest person month worked:	2
Contribution to Project:	Dr. Muniswamy organizes and coordinate weekly meetings with the lab members to ensure the incorporation of all data into a cohesive conceptual model. Dr. Muniswamy conceived and designed the study. He analyzed and interpreted experimental data and wrote the manuscript.
Funding Support:	R01 GM109882; R01GM135760; R01HL142673

Name:	Cassidy Daw
Project Role:	Graduate Research Assistant
Researcher Identifier (e.g. ORCID ID):	0000-0002-3441-0425
Nearest person month worked:	3
Contribution to Project:	Miss Daw was responsible for molecular characterization of the proposed mouse models and their breeding. She performed experiments to understand molecular mechanisms of mitochondrial Ca2+ uptake with emphasis on the effects of Ca2+ on transcription factor activation during vascular inflammation and on protein-protein interactions.

Funding Support:	T32 Training Grant

Name:	Venkata Soundarya Kandala
Project Role:	Research Assistant
Researcher Identifier (e.g. ORCID ID):	0000-0002-3776-7737
Nearest person month worked:	6
Contribution to Project:	Miss Kandala was responsible for molecular characterization of the proposed mouse models, maintenance of animal colony and their breeding, surgical procedures and vascular inflammation assessment.
Funding Support:	N/A

Name:	Karthik Ramachandran (no change)
Project Role:	Postdoctoral Research Fellow
Researcher Identifier (e.g. ORCID ID):	0000-0003-3673-3559
Nearest person month worked:	4
Contribution to Project:	Dr. Ramachandran primarily performed confocal imaging experiments linking store-operated Ca2+ entry, mitochondrial Ca2+ uptake, mROS generation, and mitochondrial functional studies.
Funding Support:	R01GM109882; R01HL086699

Name:	Manigandan Venkatesan
Project Role:	Postdoctoral Research Fellow
Researcher Identifier (e.g. ORCID ID):	0000-0003-0044-4472

Nearest person month worked:	3
Contribution to Project:	Upon joining my laboratory as a postdoctoral fellow, Dr. Venkatesan learned a big deal of confocal imaging, mitochondrial bioenergetics analysis, biochemical studies to identify the SOCe components like Ora1 and STIM1. During his period in the DOD program, he assessed the mitochondrial oxygen consumption rate, mitochondrial membrane potential and phenotype by confocal imaging and analysis using ImageJ software.
Funding Support:	R01GM109882; R01HL086699

Name:	Neelanjan Vishnu
Project Role:	Postdoctoral Research Fellow
Researcher Identifier (e.g. ORCID ID):	0000-0001-6395-4686
Nearest person month worked:	2
Contribution to Project:	Upon joining my laboratory as a postdoctoral fellow, Dr. Vishnu conducted SOCe component STIM1 redistribution after stimulation with various agonists that trigger ER Ca2+ depletion using confocal microscope. He has performed a correlative analysis to determine the colocalization of STIM1 with ER marker Sec61b that reveals the ER remodelling. Additionally, he conducted the Ca2+ induced transcription factor NFkB translocation using confocal system. Currently, he is learning how to characterize ion channel properties using biophysical, biochemical and cell biological approaches.
Funding Support:	R01GM109882; R01HL086699

Has there been a change in the active other support of the PD/PI(s) or senior/key personnel since the last reporting period?

Nothing to report.

b. **What other organizations were involved as partners?**

N/A

8. **SPECIAL REPORTING REQUIREMENTS**
    a. **COLLABORATIVE AWARDS:** This is a unique progress report submitted by Partnering PI, Madesh Muniswamy.
    b. **QUAD CHARTS:** N/A
9. **APPENDICES:** N/A